ELSEVIER

International Journal of Heat and Fluid Flow 19 (1998) 187–192

International Journal of HEAT AND FLUID FLOW

Direct numerical simulations of heat transfer by solid particles suspended in homogeneous isotropic turbulence

Yohei Sato [a,*], Emmanuel Deutsch [b], Olivier Simonin [b,c]

[a] Department of Mechanical Engineering, Faculty of Science and Technology, Keio University, 3-14-1 Hiyoshi, Kohoku-ku, Yokohama 223, Japan
[b] Direction des Études et Recherches, Laboratoire National d'Hydraulique, Electricité de France, 6, quai Watier, 78400 Chatou, France
[c] Institut de Mécanique des Fluides, Institut National Polytechnique/ENSEEIHT, Allee du Professor Camille Soula, 31400 Toulouse, France

Received 8 August 1997; accepted 25 October 1997

Abstract

The mechanism of two-phase heat and turbulent transport by small solid particles suspended in a gas flow was investigated by direct numerical simulation in decaying isotropic turbulence with or without a mean temperature gradient. The effect of fluid mean temperature gradient on heat transfer between dispersed and gas phases was examined. Velocity and temperature fields were solved by the pseudospectral method with 128^3 grid points. The behavior of 8,192 particles was time advanced by using the motion and energy equations. The imposed temperature gradient in the fluid affected the Lagrangian autocorrelation coefficient of the fluid temperature along the particle path which decreased more rapidly than that of the particle temperature. The particle temperature fluctuation correlated well with the particle velocity in the direction of the imposed temperature gradient, which was proportional to the magnitude of the gradient.

Keywords: Heat transfer; Gas–solid turbulent flow; Direct numerical simulation; Lagrangian statistics

Notation

Roman

c_p	particle specific heat
C_D	coefficient of drag $(= (24/\mathrm{Re}_p)(1 + 0.15\mathrm{Re}_p^{0.687}))$
d_p	particle diameter
$E(\kappa)$	energy spectrum
$E_\theta(\kappa)$	temperature spectrum
k	turbulence kinetic energy
N	grid size
Nu	Nusselt number $(= 2 + 0.55\mathrm{Re}_p^{1/2}\mathrm{Pr}^{1/3})$
p	pressure
q_0^2	initial twice turbulence kinetic energy
Pr	Prandtl number
r	mechanical dissipation to thermal dissipation ratio
Re	Reynolds number based on reference length and velocity $(= v/UL)$
Re_λ	Taylor-scale Reynolds number
$R\theta^L$	Lagrangian autocorrelation coefficient of temperature
t	dimensionless time (normalized by reference length and velocity)
u	velocity fluctuation
$\boldsymbol{u}_f$	fluid velocity vector
$\boldsymbol{u}_p$	particle velocity vector
$\langle u_{p_i}\theta_p\rangle$	correlation between particle velocity and temperature fluctuations
x_i	ith direction

Greek

α	thermal diffusivity of fluid
ε	homogeneous dissipation rate
ε_θ	temperature dissipation rate
η	Kolmogorov microscale $(= (v^3/\varepsilon)^{1/4})$
η_θ	temperature microscale $(= (\alpha^3/\varepsilon)^{1/4})$
θ	temperature fluctuation
$\langle\Theta\rangle$	mean temperature
κ	wave number
λ	Taylor microscale
λ_f	thermal conductivity of fluid
v	kinematic viscosity
ρ	density
τ	time

Subscripts

0	$t = 0$
f	fluid
f@p	fluid along particle path
p	particle

1. Introduction

Knowledge of the behavior of discrete particles in turbulent flow has attracted increased interest, as turbulent flows laden

* Corresponding author. E-mail: yohei@mh.sd.keio.ac.jp.

0142-727X/98/$19.00
PII: S0142-727X(97)10023-6

with solid particles are a common occurrence in both nature and technology. An increase in scalar diffusion by solid particles is one of the most fascinating aspects of turbulence control and protecting environment. Prediction of these flows is of importance because turbulent flows laden with particles occur in many technologically important areas and nature. It should be remembered that adding particles to a single-phase flow dramatically complicates characterization of the flow and renders the traditional empirical methodology for single-phase flow far from complete.

Direct numerical simulation (DNS) has recently become a powerful supplement to experimental investigations of turbulence in complex phenomena and has been shown to be capable of accurately reproducing the physics of moderate-Reynolds-number turbulent flows. DNSs have been used to study particle dispersion (Riley and Patterson, 1974; Squires and Eaton, 1991; Elghobashi and Truesdell, 1992; Wang and Maxey, 1993) and turbulence modification by small particles (Squires and Eaton, 1990; Elghobashi and Truesdell, 1993). None of the studies, however, investigated scalar transport by solid particles suspended in turbulent flows by direct numerical simulations.

For engineering applications turbulence models must be considered and, to this day, they represent the most economically feasible approach to analyzing dispersed two-phase turbulent flows. Numerical studies can be developed either by an Eulerian–Eulerian model (Elghobashi and Abou-Arab, 1983; Picart et al., 1986; Simonin et al., 1993) or an Eulerian–Lagrangian model (Berlemont et al., 1990; Sato, 1996). These models require information which cannot be obtained from experiments. Thus, the difficult-to-measure model terms must be found from the full Navier–Stokes, scalar and particle motion equations solved without modeling.

In the present study direct numerical simulations are used to investigate, for the first time, heat and turbulent transport by small solid particles suspended in homogeneous isotropic turbulence with or without an imposed mean temperature gradient. The purpose of this work is to consider important questions left unanswered by experimental studies in the literature and to construct a database for the refinement of both the Eulerian–Eulerian and the Eulerian–Lagrangian models. Most of the simulations in this study were performed on a 128^3 grid, yielding values of Taylor-scale Reynolds number from 54 to 40 and a Prandtl number of 0.7.

This study is the first publication from an ongoing research program related to heat, mass and turbulent transport in the presence of dispersed phase, i.e. solid particles and droplets, in turbulent flows. The paper describes and discusses the effect of a mean temperature gradient on the Lagrangian autocorrelation of temperature, the correlation between particle velocity and temperature fluctuations and temperature-fluctuation variances.

2. Overview of the simulations

2.1. Pseudospectral method

The present simulations solved the following forms of the continuity, Navier–Stokes and scalar equations

$$\frac{\partial u_{\mathrm{f}_i}}{\partial x_i} = 0, \tag{1}$$

$$\frac{\partial u_{\mathrm{f}_i}}{\partial t} + u_{\mathrm{f}_j}\frac{\partial u_{\mathrm{f}_i}}{\partial x_j} = -\frac{\partial p}{\partial x_i} + \frac{1}{\mathrm{Re}}\frac{\partial^2 u_{\mathrm{f}_i}}{\partial x_j \partial x_j}, \tag{2}$$

$$\frac{\partial \theta_{\mathrm{f}}}{\partial t} + u_{\mathrm{f}_j}\frac{\partial \theta_{\mathrm{f}}}{\partial x_j} = \frac{1}{\mathrm{RePr}}\frac{\partial^2 \theta_{\mathrm{f}}}{\partial x_j \partial x_j} - u_{\mathrm{f}_2}\frac{\partial \langle \Theta_{\mathrm{f}} \rangle}{\partial x_2}, \tag{3}$$

applicable to an incompressible fluid on a three-dimensional grid. In wave-number space the grid represents the integer wave numbers $\kappa_i = \pm n_i$ where $n_i = 0, 1, 2, \ldots, N/2$ for $i = 1, 2, 3$. The pseudospectral method advances the solution in time in wave-number space, i.e., the spatial-derivative terms in the Navier–Stokes and scalar equations are computed in wave-number (Fourier) space, while the non-linear terms are computed in physical space, requiring discrete fast Fourier transforms (FFTs) to transform the fields back and forth between physical space and wave number space. The aliasing errors incurred in the FFTs are almost completely removed by phase shifting and truncation techniques. The truncation results in a maximum significant wave number, $\kappa_{\max}$, of $\sqrt{2}N/3$. The solution was obtained on a cubical uniform grid with N^3 grid points and a cube with sides of length 2π in physical space. For further details of the method, see Canuto et al. (1988).

The time-stepping scheme employs an explicit second-order Runge–Kutta method with an integrating factor technique. Time-stepping errors are small as long as the Courant number (cfl) is not greater than 1.0. Courant numbers greater than unity are found to cause a marked increase in the time-stepping errors (Eswaran and Pope, 1988). The Courant number was chosen to be 0.5 in the present simulations.

2.2. Particle tracking method

The ratio of fluid density to particle density is assumed to be negligible; therefore only the drag force was considered in the equation of particle motion:

$$\frac{\mathrm{d}u_{\mathrm{p}_i}}{\mathrm{d}t} = -\frac{3}{4}\frac{C_{\mathrm{D}}}{d_{\mathrm{p}}}\frac{\rho_{\mathrm{f}}}{\rho_{\mathrm{p}}}\left(u_{\mathrm{p}_i} - u_{\mathrm{f}_i}\right)\left|\boldsymbol{u}_{\mathrm{p}} - \boldsymbol{u}_{\mathrm{f}}\right|. \tag{4}$$

It is assumed that the concentration of particles is small enough for particle–particle interactions to be negligible and the turbulence is not modified by the presence of the particles. It should be remembered that gravity is removed in order to avoid the crossing-trajectories effect.

The instantaneous particle temperature, θ_{p}, is obtained by integrating the energy equation:

$$\frac{\mathrm{d}\theta_{\mathrm{p}}}{\mathrm{d}t} = -\frac{6\lambda_{\mathrm{f}}\mathrm{Nu}}{d_{\mathrm{p}}^2 \rho_{\mathrm{p}} c_{\mathrm{p}}}\left(\theta_{\mathrm{p}} - \theta_{\mathrm{f}}\right), \tag{5}$$

where Nu is the Nusselt number. It is also assumed that the particle enthalpy does not affect the temperature flow field. Eqs. (4) and (5) were time advanced using second-order Runge–Kutta.

Interpolation is required to obtain fluid information at a particle point. In the present study third-order accurate Lagrange polynominals were used to interpolate velocities and temperatures at grid points (Deutsch, 1990; Squires and Eaton, 1991).

Particles were uniformly injected within the computational box. All the simulations in the present study used 8,192 particles. The initial velocity was assumed to be equal to the fluid velocity at the same location and the initial temperature was set as the non-dimensionalized temperature of unity ($=300$ K).

3. Results and discussion

3.1. Properties of the Eulerian field

The parameters of decaying isotropic turbulence by DNS are summarized in Table 1 where Re_λ is the Reynolds number

Table 1
Fluid flow parameters

Grid size	N	128
Reynolds number	Re_λ	54.3–39.7
Courant number	cfl	0.5
Kinematic viscosity	$\nu = 1/\mathrm{Re}$ [a]	0.001
Prandtl number	Pr	0.71
Density	ρ_f	1.17 kg/m^3
Thermal conductivity	λ_f	2.61×10^{-2} J/m s K
Mean temperature gradient	$\partial\langle\Theta_\mathrm{f}\rangle/\partial x_2$	0.0, 1.0, 10.0
Kolmogorov microscale	η [a]	0.0166–0.0391
Taylor microscale	λ [a]	0.241–0.466
Eulerian timescale	$T_E = k/\varepsilon$	5.80–21.7
	q_0^2	3
	κ_peak	8
	σ	4

[a] Reference length and velocity were chosen to be 0.01 m and 1.0 m/s, respectively.

based on the Taylor microscale. The imposed mean temperature gradient was chosen to be unity and ten.

The initial energy spectrum for both fluid velocity and temperature was specified following the procedure of Batchelor et al. (1992) and Chasnov (1994). The initial spatial energy spectrum was taken to be of the form

$$E(\kappa) = E_\theta(\kappa) = \frac{\sigma^{\sigma+1/2}}{(1 \times 3 \times \cdots \times \sigma - 1)}\sqrt{\frac{2}{\pi}}q_0^2 \times \frac{\kappa^\sigma}{\kappa_\mathrm{peak}^{\sigma+1}}\exp\left\{-\frac{\sigma}{2}\left(\frac{\kappa}{\kappa_\mathrm{peak}}\right)^2\right\}, \quad (6)$$

where κ_peak is the wave number at which $E(\kappa)$ is maximum and σ is a parameter. Fig. 1 displays the spatial energy spectra of decaying isotropic turbulence. The initial spectrum is unrealistic, but as the flow develops the energy is redistributed to both low and high wave numbers and the Reynolds number decreases. In isotropic decay the resolution of the small scales is judged by the shape of the spectrum at high wave numbers.

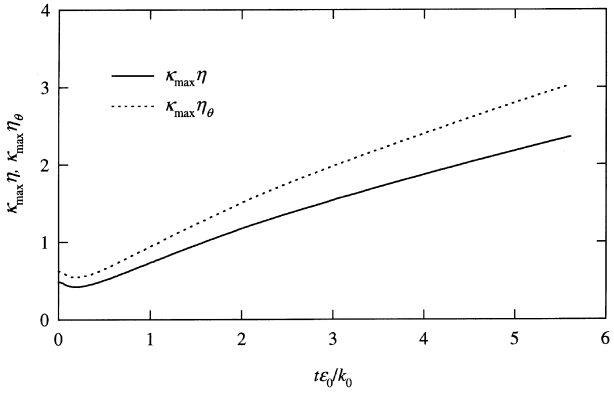

Fig. 2. Spatial resolution of the Kolmogorov scale in decaying isotropic turbulence.

As a rule of thumb it is required that the numerical cut-off wave number be at or beyond $\kappa_\mathrm{max}\eta = 1$, shown in Fig. 2, where η is the Kolmogorov microscale. The time axis of all figures represented in this section has been made dimensionless using the initial turbulence kinetic energy, k_0, and the initial homogeneous dissipation rate, ε_0.

The temperature spectra without and with the imposed gradient are displayed in Fig. 3. The initial spectra were set to equal to Eq. (6). Good resolution is obtained when the parameter $\kappa_\mathrm{max}\eta_\theta = 1$ is greater than or equal to unity, shown in Fig. 2, where η_θ is the temperature microscale (Tennekes and Lumley, 1972).

The ability of DNS to resolve the motion at the smallest turbulence scale is judged by the dimensionless quantity $\kappa_\mathrm{max}\eta$ shown in Fig. 2. Yeung and Pope (1988) indicated that the smallest scales are captured when $\kappa_\mathrm{max}\eta = 1$. When the value of $\kappa_\mathrm{max}\eta$ is unity, $\kappa_\mathrm{max}\eta_\theta$ is already greater than unity, which means that all the scales are resolved in the present DNS.

The time development of mechanical dissipation to thermal dissipation ratio, defined by

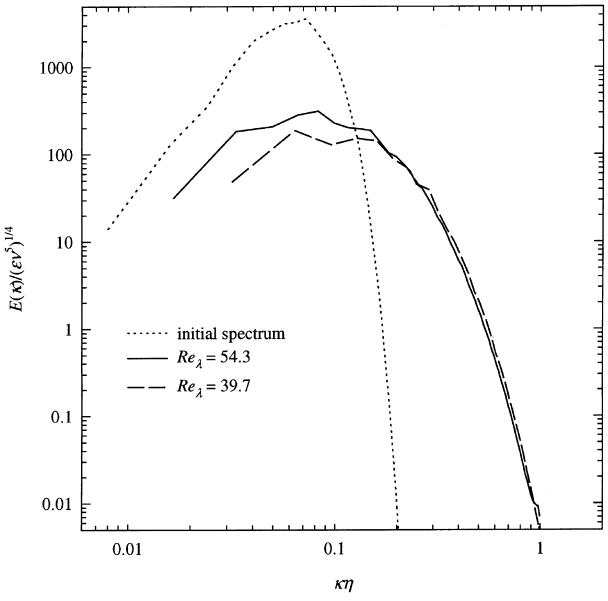

Fig. 1. Three-dimensional spatial energy spectra in decaying isotropic turbulence.

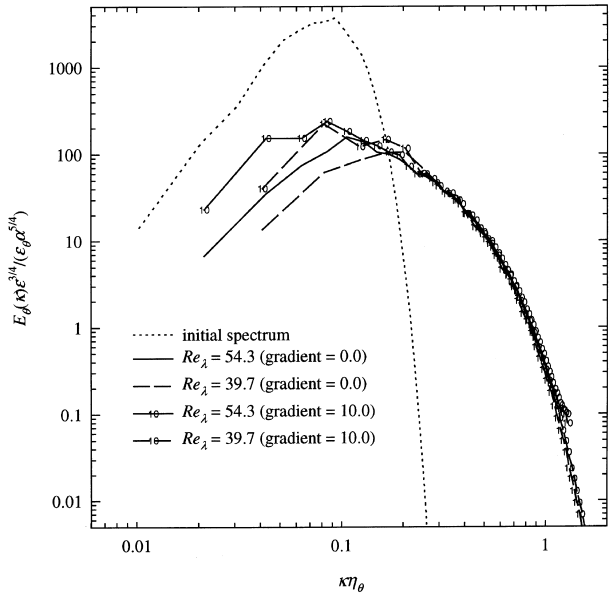

Fig. 3. Temperature spectra in decaying isotropic turbulence without and with a mean temperature gradient.

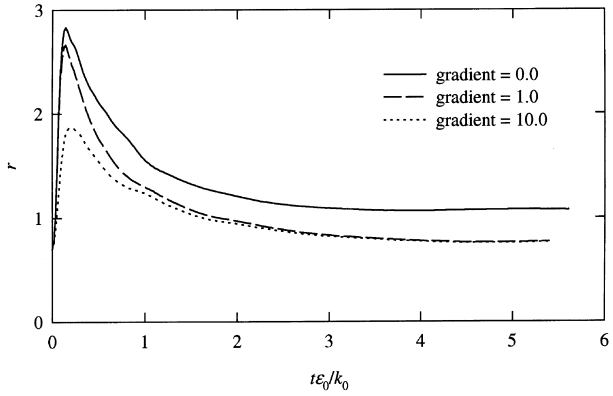

Fig. 4. Time development of mechanical dissipation to thermal dissipation ratio in decaying isotropic turbulence.

$$r = \frac{2k/\varepsilon}{\langle\theta^2\rangle/\varepsilon_\theta}, \tag{7}$$

is depicted in Fig. 4. The dissipation ratio with the mean temperature gradient decreases faster than that without the gradient which has an asymptotic value of unity with respect to time. Warhaft and Lumley (1978) review a number of heated grid experiments and find r values of 0.6–2.4.

Profiles of the non-dimensional Taylor microscale and Kolmogorov microscale with respect to time are shown in Fig. 5. These scales were calculated directly from the spectra of the energy and dissipation. The ratio of the Taylor to Kolmogorov scales indicates the range 12–15, which is denoted by the following equation (Tennekes and Lumley, 1972):

$$\frac{\lambda}{\eta} = 15^{1/4}\mathrm{Re}_\lambda^{1/2} \approx 14. \tag{8}$$

3.2. Initial condition of particles

After the turbulence had developed to eliminate the physical characteristics of the initial conditions the particles were time advanced using Eqs. (4) and (5). The particles were released after the skewness of the velocity derivative had reached a threshold value corresponding to developed turbulence. The value of the skewness corresponding to developed turbulence is approximately −0.4 to −0.5 (Tavoularis et al., 1978; Squires and Eaton, 1991; Elghobashi and Truesdell, 1992), shown in Fig. 6. Table 2 is a summary of the particle properties used in the present DNS.

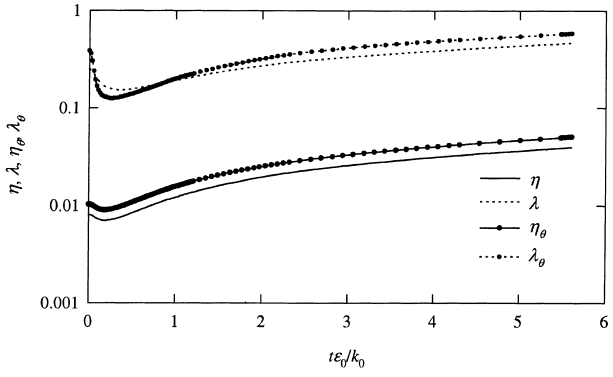

Fig. 5. Time development of the Kolmogorov lengthscale and Taylor microscale in decaying isotropic turbulence without a mean temperature gradient.

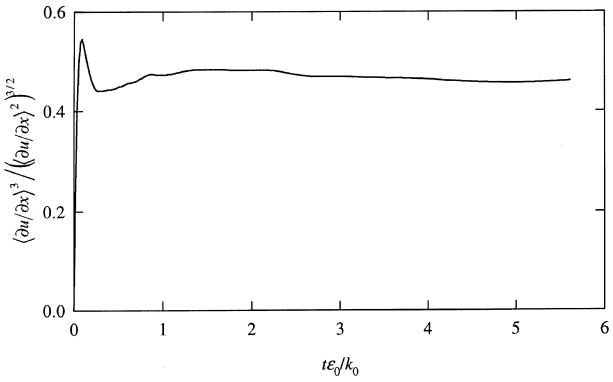

Fig. 6. Time development of the skewness of the fluid velocity derivatives in decaying isotropic turbulence.

It is important that Lagrangian statistics measured for the particles be computed only after the particles have become independent of their initial conditions. Riley and Patterson (1974) were the first to use the time of occurrence of the peak of the mean-square relative velocity between fluid particles in order to indicate the time at which the particles had adjusted to the decaying turbulence. Squires and Eaton (1991) and Elghobashi and Truesdell (1992) indicated in their DNS studies that the Lagrangian statistics were computed after the mean-square relative velocity had obtained its maximum value. However, in the present study the maximum value is sensitive to the correlation between the particle velocity and the temperature fluctuations. The influence of the initial conditions was completely eliminated to obtain the Lagrangian statistics and throughout the remainder of the paper the time origin, $t=0$, of all the statistical quantities is the time when the Taylor-scale Reynolds number took a value of 54.

3.3. Lagrangian autocorrelation function

The Lagrangian autocorrelation coefficient of temperature without and with the imposed mean temperature gradient is shown in Fig. 7(a) and (b), respectively. The coefficient of particle temperature is defined as

$$R\theta_{\mathrm{p}}^L(t_0,\tau) = \frac{\langle\theta_{\mathrm{p}}(t_0)\theta_{\mathrm{p}}(t_0+\tau)\rangle}{\langle\theta_{\mathrm{p}}(t_0)^2\rangle^{1/2}\langle\theta_{\mathrm{p}}(t_0+\tau)^2\rangle^{1/2}}. \tag{9}$$

The normalization lessens the effect on the correlation of the reference time of measurement, $t=0$ (Squires and Eaton, 1991). The Lagrangian autocorrelation coefficient of fluid temperature along the particle path is computed as

$$R\theta_{\mathrm{f@p}}^L(t_0,\tau) = \frac{\langle\theta_{\mathrm{f@p}}(t_0)\theta_{\mathrm{f@p}}(t_0+\tau)\rangle}{\langle\theta_{\mathrm{f@p}}(t_0)^2\rangle^{1/2}\langle\theta_{\mathrm{f@p}}(t_0+\tau)^2\rangle^{1/2}}. \tag{10}$$

The memory of the particle of its previous temperature diminishes as the Reynolds number decreases. The temperature of the fluid along the particle path loses memory more rapidly than the particle. It can be observed from these figures that the autocorrelation of the particle temperature does not seen to be affected by the imposed gradient. At short times the fluid temperature autocorrelation decreases rapidly in the case without the gradient.

The functional form for the velocity autocorrelation of fluid along the particle path,

Table 2
Particle properties

Mean diameter	d_p	[μm]	50.0
Density	ρ_p	[kg/m^3]	8,800
Specific heat	c_p	[J/(kg K)]	386
Particle time constant	τ_p	[ms]	104
Gas–particle temperature transfer characteristic time			
	τ_{θ_p}	[ms]	21.7
Lengthscale ratio	d_p/η	[−]	0.301–0.127
Timescale ratio	T_E/τ_p	[−]	0.557–2.08
	T_E/τ_{θ_p}	[−]	2.67–10.0

$$R^L_{f@p_{ij}}(\tau) = \exp\left[\frac{-\tau}{(m^2+1)\tau^L_{f@p_{ij}}}\right] \times \cos\left[\frac{m\tau}{(m^2+1)\tau^L_{f@p_{ij}}}\right], \quad (11)$$

has been proposed by Gouesbet et al. (1984), where $\tau^L_{f@p_{ij}}$ is the Lagrangian integral timescale tensor of fluid along the particle path. For increasing values of the loop parameter, m, the correlation function will have negative loops. From Fig. 7(a) and (b), however, the autocorrelation of the fluid temperature has no negative loop. If the functional form given by Eq. (11) can be applied to the fluid temperature autocorrelations, the value of m must be less than unity.

3.4. Temperature fluctuation variance

The time development of the temperature-fluctuation variance of the particle and the fluid along the particle path without an imposed temperature gradient is displayed in Fig. 8. All the quantities decreased with respect to time in velocity and temperature decaying turbulence. It can be observed that the fluid temperature variance decreases slightly faster than that of particle, due to the fact that the particle temperature variance decays with $1/\tau_{\theta_p}$ rather than $1/T_E$ for the fluid. The effect may also be due to increasing values of turbulent macroscales, i.e., T_E and T_L. A significant effect of the imposed gradient on temperature variances is observed in Fig. 9 when the temperature gradient was added. The temperature fluctuation variance of the fluid along the particle path has constant values with respect to time, while the particle temperature variance increased with decreasing value of the Reynolds number and reached the asymptotic values.

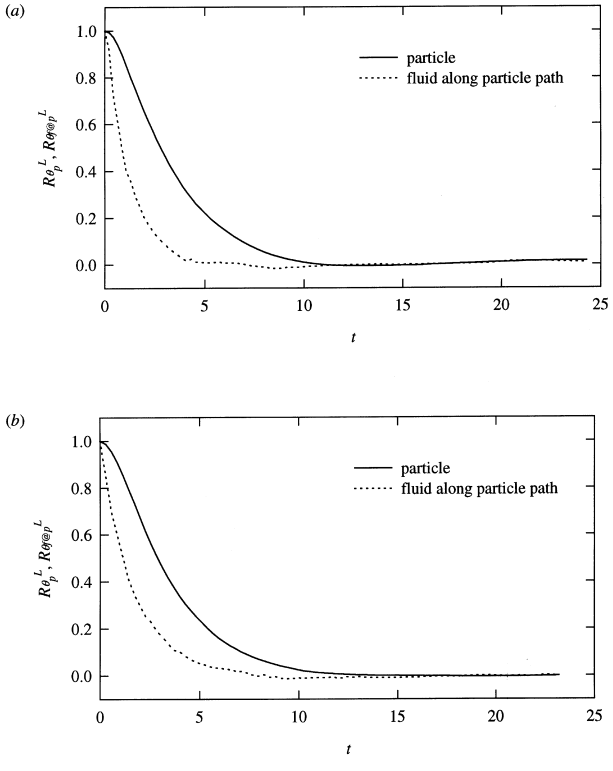

Fig. 7. Lagrangian autocorrelation coefficient of temperature: (a) without a mean temperature gradient; (b) with a mean temperature gradient of unity.

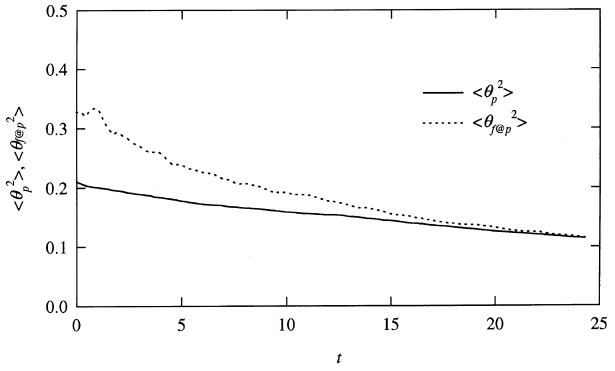

Fig. 8. Time development of temperature-fluctuation variances without a mean temperature gradient.

3.5. Temperature turbulent flux

In turbulence modeling of particle-laden flows, the correlations related to the particle behavior are evaluated by using the

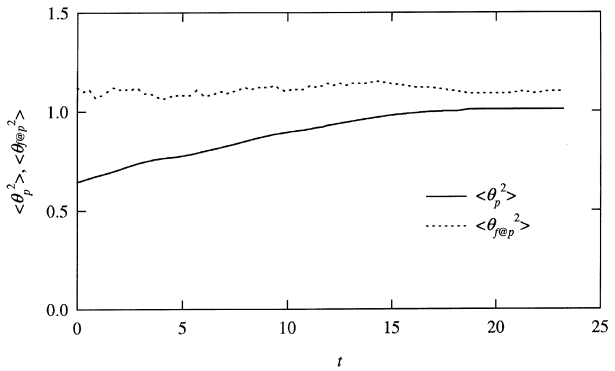

Fig. 9. Time development of temperature-fluctuation variances with a mean temperature gradient of unity.

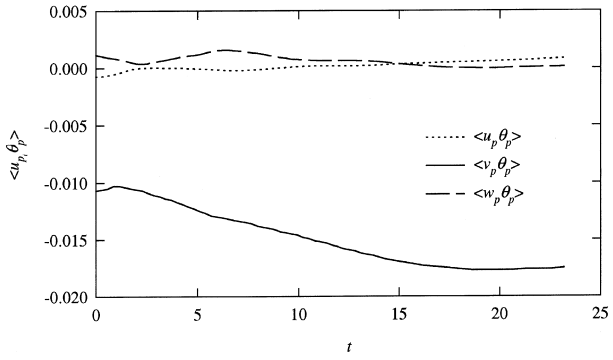

Fig. 10. Time development of correlation between particle velocity and temperature fluctuations with a mean temperature gradient of unity.

gradient-diffusion hypothesis or the transport equations (Simonin, 1996); thus quantitative information is required. Fig. 10 depicts the time development of the correlation between the particle velocity and temperature fluctuations with the gradient of unity. It is observed that the mean temperature gradient contributes to the particle temperature fluctuation in the direction of the gradient which is proportional to the magnitude of the imposed gradient. As can be seen from the figure the other correlations have zero values which were not affected by the initial condition.

4. Conclusions

Direct numerical simulations were performed to investigate heat and turbulent transport by solid particles suspended in decaying isotropic turbulence with or without an imposed fluid mean temperature gradient. The present study focused on the effect of the temperature gradient on the Lagrangian statistics of the particle and the fluid along the particle path in the range of Taylor-scale Reynolds numbers from 54 to 40. The imposed temperature gradient affected the Lagrangian autocorrelation coefficient of the fluid temperature along the particle path which decreased more rapidly than that of the particle temperature. The particle temperature fluctuation correlated well with the particle velocity in the direction of the imposed temperature gradient and was proportional to the magnitude of the gradient. With the mean temperature gradient the particle temperature fluctuation variance increased with time.

The present study shows the feasibility of DNS from a dynamic point of view, with the imposed mean temperature gradient yielding non-zero turbulent fluxes. The simulations allow us to study not only heat transfer between the gas and the solid particles, but also heat and turbulent transport in the dispersed phase.

The present direct numerical simulations were conducted in decaying isotropic turbulence. The next step, which involves studying the behavior in forced isotropic turbulence and at high Reynolds number by using large eddy simulations, is currently under way.

Acknowledgements

The first author is pleased to acknowledge the Japan Society for the Promotion of Science and Professor Koichi Hishida of Keio University for their help. This work was supported by the Grant-in-Aid of the Japanese Ministry of Education, Science and Culture (Grant No. 4940).

References

Batchelor, G.K., Canuto, V.M., Chasnov, J.R., 1992. Homogeneous buoyancy-generated turbulence. J. Fluid Mech. 235, 349–378.

Berlemont, A., Desjonqueres, P., Gouesbet, G., 1990. Particle Lagrangian simulation in turbulent flows. Int. J. Multiphase Flow 16, 19–34.

Canuto, J.R., Hussaini, M.Y., Quarteroni, A., Zang, T.A., 1988. Spectral Methods in Fluid Dynamics. Springer, Berlin.

Chasnov, J.R., 1994. Similarity states of passive scalar transport in isotropic turbulence. Phys. Fluids 6, 1036–1051.

Deutsch, E., 1990. Dispersion de particules dans une turbulence homogene isotrope stationnaire calculee par simulation numerique directe des grandes echelles. Electricité de France.

Elghobashi, S., Abou-Arab, T.W., 1983. A two-equation turbulence model for two-phase flows. Phys. Fluids 26, 931–938.

Elghobashi, S., Truesdell, G.C., 1992. Direct simulation of particle dispersion in a decaying isotropic turbulence. J. Fluid Mech. 242, 655–700.

Elghobashi, S., Truesdell, G.C., 1993. On the two-way interaction between homogeneous turbulence and dispersed solid particles I: Turbulence modification. Phys. Fluids A 5, 1790–1801.

Eswaran, V., Pope, S.B., 1988. An examination of forcing in direct numerical simulations of turbulence. Computers and Fluids 16, 257–278.

Gouesbet, G., Berlemont, A., Picart, A., 1984. Dispersion of discrete particles by continuous turbulent motions. Extensive discussion of the Tchen's theory, using a two-parameter family of Lagrangian correlation functions. Phys. Fluids 27, 827–837.

Picart, A., Berlemont, A., Gouesbet, G., 1986. Modeling and predicting turbulence fields and the dispersion of discrete particles transported by turbulent fields. Int. J. Multiphase Flow 12, 237–261.

Riley, J.J., Patterson, G.S., 1974. Diffusion experiments with numerically integrated isotropic turbulence. Phys. Fluids 17, 292–297.

Sato, Y., 1996. Turbulence Structure and Modeling of Dispersed Two-Phase Flows. Ph.D. Dissertation, Keio University.

Simonin, O., 1996. Combustion and Turbulence in Two-Phase Flows. Lecture Series 1996-02, von Karman Institute for Fluid Dynamics.

Simonin, O., Deutsch, E., Minier, J.P., 1993. Eulerian prediction of the fluid/particle correlated motion in turbulent two-phase flows. Appl. Scientific Res. 51, 275–283.

Squires, K.D., Eaton, J.K., 1990. Particle response and turbulence modification in isotropic turbulence. Phys. Fluids A 2, 1191–1203.

Squires, K.D., Eaton, J.K., 1991. Measurements of particle dispersion obtained from direct numerical simulations of isotropic turbulence. J. Fluid Mech. 226, 1–35.

Tavoularis, S., Bennett, J.C., Corrsin, S., 1978. Velocity derivative skewness in small Reynolds number, nearly isotropic turbulence. J. Fluid Mech. 88, 63–69.

Tennekes, H., Lumley, J.L., 1972. A First Course in Turbulence. MIT Press, MA.

Wang, L.P., Maxey, M.R., 1993. Settling velocity and concentration distribution of heavy particles in homogeneous isotropic turbulence. J. Fluid Mech. 256, 27–68.

Warhaft, Z., Lumley, J.L., 1978. An experimental study of the decay of temperature fluctuations in grid-generated turbulence. J. Fluid Mech. 88, 659–684.

Yeung, P.K., Pope, S.B., 1988. An algorithm for tracking fluid particles in numerical simulations of homogeneous turbulence. J. Comp. Phys. 79, 373–415.